JOURNAL OF GEOPHYSICAL RESEARCH, VOL. 105, NO. A12, PAGES 27,195–27,215, DECEMBER 1, 2000

Improved solar Lyman α irradiance modeling from 1947 through 1999 based on UARS observations

Thomas N. Woods,[1] W. Kent Tobiska,[2] Gary J. Rottman,[1] and John R. Worden[3]

Abstract. The solar Lyman α radiation is the brightest solar vacuum ultraviolet (VUV: λ < 200 nm) emission, and this radiation is deposited in Earth's atmosphere above 70 km. The Lyman α irradiance and its variability are therefore important for many studies of the Earth's upper atmosphere. A long-term data set of the solar Lyman α irradiance from 1947 through 1999 is constructed using the measurements from the Atmospheric Explorer E (AE-E), the Solar Mesospheric Explorer (SME), and the Upper Atmosphere Research Satellite (UARS) along with predictions from proxy models to fill in data gaps and to extrapolate back to 1947. The UARS measurement is used as the reference, and the AE-E and SME measurements and the proxy models are adjusted to agree with the UARS values. The estimated 1-σ uncertainty for this long-term Lyman α time series is 10%. The average solar rotation (27-day) variability in Lyman α is 9% from this composite times series, and the solar rotation variability averaged over 2 years at solar minimum and maximum conditions is 5 and 11%, respectively. The average solar cycle (11-year) variability is a factor of 1.5 when the data are smoothed over 2 years, and the extreme Lyman α variability is a factor of 2.1. The Lyman α irradiances averaged over 2 years during solar minimum and maximum conditions are 3.7 and 5.6 x 10^{11} photons s^{-1} cm^{-2}, respectively. The proxy models include three components to better fit the UARS measurements; nonetheless, there remain differences between the proxy models and the observed Lyman α irradiance, which are related to the source of the Lyman α radiation being different than that for the proxies. The available proxies are primarily chromospheric and coronal emissions, whereas the Lyman α variability is manifested more in the transition region. It is shown that emissions throughout the chromosphere, transition region, and corona vary differently mainly because their contrasts for active network and plage components are different. A transition region proxy is needed to improve the empirical proxy models of solar irradiance, and this composite Lyman α time series could serve as a proxy for other transition region emissions.

1. Introduction

The bright solar Lyman α radiation of the hydrogen emission at 121.6 nm is an important ultraviolet (UV) source of energy throughout the solar system. For the Earth the solar Lyman α photons penetrate into the mesosphere and deposit their energy mainly by molecular oxygen dissociation in the 70-100 km region. In addition, the solar Lyman α radiation dissociates water in the mesosphere and ionizes nitric oxide to form the ionospheric *D* layer between 80 and 110 km. Because the solar Lyman α radiation is the dominant component in the solar spectrum to drive atmospheric changes in the 70-110 km region, it plays an important role in the chemistry of the minor species such as water vapor, ozone, and nitric oxide [*Frederick*, 1977; *Brasseur and Simon*, 1981]. Therefore accurate measurements of the solar Lyman α irradiance are important for studies of the ionosphere and mesospheric chemistry.

The determination of the hydrogen density in the heliosphere, comets, and planetary atmospheres is largely based on measuring the brightness at Lyman α caused by the resonant scattering of the solar Lyman α emission. In particular, the column density of hydrogen is derived by dividing the measured brightness of the H I Lyman α emission by the g factor, or fluorescence efficiency, and the g factor is based on well-known atomic parameters, such as the emission's oscillator strength, and the solar irradiance [*Meier*, 1995]. Consequently, the accuracy of the hydrogen abundance is directly dependent on the accuracy of the Lyman α brightness measurement and on the accuracy of the solar Lyman α irradiance, both intensity and line profile. Often there are not correlative measurements of the solar Lyman α irradiance, so estimates or measurements at different times are instead used to analyze the hydrogen abundance in these solar system studies. The long-term, continuous time series of Lyman α irradiance presented here will address this issue by providing accurate solar Lyman α irradiances since 1947, at about the time when space-based measurements of the H I Lyman α emissions within the solar system began.

In order to make a long-term time series of the solar Lyman α irradiance, models of the Lyman α irradiance are needed for time periods when measurements are not available. Understanding the sources of the Lyman α radiation is important for developing accurate models of the Lyman α irradiance. The Lyman α irradiance has both chromospheric and transition region sources [*Vernazza et al.*, 1981], and the

[1]Laboratory for Atmospheric and Space Physics, University of Colorado, Boulder.
[2]Federal Data Corporation, Jet Propulsion Laboratory, Pasadena, California.
[3]Atmospheric and Environmental Research Inc., Cambridge, Massachusetts.

Paper number 2000JA000051.
0148-0227/00/2000JA000051$09.00

radiative process of this emission complicates the emergence of the Lyman α radiation. The main component of Lyman α irradiance is the central 0.1 nm line core, which is formed at a temperature of ~40,000 K in the transition region [*Fontenla et al.*, 1991]. The Lyman α line width of 0.1 nm is due to radiative damping, the Stark effect (electric field broadening), and resonance broadening [*Roussel-Dupré*, 1983; *Vernazza et al.*, 1981]. The transition region Lyman α core emission, besides contributing to the irradiance output, radiates down into the chromosphere where coherent scattering leads to partial redistribution of the Lyman α radiation into broad wings [*Roussel-Dupré*, 1983; *Vernazza et al.*, 1981]. The source of the Lyman α wing goes deeper into the chromosphere as one observes farther from the line center. The source function for the Lyman α emission as calculated by *Fontenla et al.'s* [1991] model is presented by *Woods et al.* [1995]. The source function for the quiet Sun model (model C-average cell interior) has the peak Lyman α emission near 40,000 K in the lower transition region. For the plage model (model P), the Lyman α source function has its peak higher in the transition region at a temperature of ~70,000 K and accompanied by an increase in the radiance by a factor of ~6. This shift of the source function to higher in the transition region for plages is probably the main reason why the Lyman α irradiance varies more like a transition region emission than like a chromospheric emission.

Recent progress to consolidate the past solar Lyman α irradiance measurements into a long-term composite time series includes the effort of *Woods and Rottman* [1997] and *Tobiska et al.* [1997]. These previous results only included UARS Solar Stellar Irradiance Comparison Experiment (SOLSTICE) data through 1994, which is almost 2 years before the recent solar minimum. The new results presented here include both solar cycle minimum and maximum measurements by the UARS SOLSTICE, significant improvements to the UARS SOLSTICE data processing, and a composite time series of Lyman α irradiance that fills the measurement gaps and extends the time series back almost 30 years further than the previous estimates. The improvements to the UARS SOLSTICE Lyman α irradiances are presented first, followed by the proxy models of the Lyman α irradiance that are calibrated to the UARS solar data. Then the composite of the revised measurements and proxy model predictions is presented as a single, consistent time series of the Lyman α irradiance from 1947 through 1999 with no data gaps. Finally, the sources of the Lyman α emission and of the proxies are examined in order to interpret the differences seen between the Lyman α and proxies variability.

2. Lyman α Measurements

Because of the atmospheric absorption, the solar Lyman α radiation must be measured from space. Several satellites have measured the solar Lyman α irradiance: Solrad 8 (1966), Orbiting Solar Observatory 3 (OSO 3: 1967), OSO 4 (1967-1968), OSO 5 (1969-1975), OSO 6 (1969-1970), Nimbus 3 and 4 (1969-1973), Atmospheric Explorer E (AE-E: 1977-1980), Solar Mesospheric Explorer (SME: 1981-1989), San Marco (1988), and Upper Atmosphere Research Satellite (UARS: 1991-2000). There have also been over 60 sounding rocket measurements of solar Lyman α since 1949; many of these rocket experiments were from the Air Force Geophysical Laboratory (now Phillips Laboratory), the Naval Research Laboratory, and the University of Colorado to provide an underflight calibration for the satellite measurements. Despite the underflight calibration effort, the satellite measurements of the solar Lyman α irradiance do have significant differences. These differences are partly due to using different photometric standards and to having limited on-board calibration for the pre-UARS solar instruments. Resolving these differences is important in order to combine the different data sets into a single reference and thereby to estimate long-term solar variability.

The satellite measurements used here are from the AE-E, SME, and UARS. The uncertainties for the SME Lyman α irradiances are ~40% [*Rottman*, 1981; *Mount and Rottman*, 1983], and the uncertainties for the AE-E Lyman α irradiances are ~30% [*Hinteregger et al.*, 1981]. Whereas, the uncertainty for the UARS Lyman α irradiance is 5% [*Woods et al.*, 1996]. The SME and AE-E measurements could therefore be adjusted within their respective uncertainty levels to agree with the UARS values. These uncertainties and others used elsewhere in this report are 1-σ values.

Because these three satellite missions do not overlap in time, the adjustments for the AE-E and SME data must be determined using proxy models of the Lyman α irradiance that are scaled to the UARS solar measurements. *Woods and Rottman* [1997] used proxy models involving the Penticton (Ottawa) 10.7-cm radio flux ($F10.7$) [*Tapping*, 1987], the National Oceanic and Atmospheric Administration (NOAA) Mg II core-to-wing ratio (Mg C/W) [*Heath and Schlesinger*, 1986; *Donnelly et al.*, 1994], the National Solar Observatory (NSO) He 1083-nm equivalent width (He EW) [*Harvey and Livingston*, 1992], and the Pioneer Venus (PV) Langmuir probe solar measurements (Ipe) [*Hoegy et al.*, 1993]. *Tobiska et al.* [1997] used a proxy model derived from the Lyman α sky background measurements made over two solar cycles by the PV Orbiter Ultraviolet Spectrometer (PVOUVS). The AE-E and SME adjustments from *Woods and Rottman* [1997] and from *Tobiska et al.* [1997] are very similar. Their differences arise primarily in the data chosen as the UARS Lyman α irradiance reference value. *Tobiska et al.* [1997] chose to use the measurements solely from the UARS SOLSTICE [*Rottman et al.*, 1993]. *Woods and Rottman* [1997] also used the SOLSTICE Lyman α values but modified by a factor of 0.95 to represent an average of the measurements from the two UARS instruments, SOLSTICE and Solar Ultraviolet Spectral Irradiance Monitor (SUSIM) [*Brueckner et al.*, 1993]. The 10% difference between the UARS SOLSTICE and UARS SUSIM Lyman α irradiances is within their 2-σ absolute uncertainty of 10% [*Woods et al.*, 1996].

The previous studies by *Woods and Rottman* [1997] and *Tobiska et al.* [1997] considered data only during the declining phase of solar cycle 22. This new analysis extends from solar cycle 22 maximum through solar minimum and into the rising phase of solar cycle 23. Consequently, the longer time period, coupled with improvements to the UARS SOLSTICE data processing algorithms and calibration parameters, prescribes different scaling factors for the AE-E and SME Lyman α irradiances.

For the long-term composite Lyman α time series presented here, the UARS SOLSTICE version 13 Lyman α irradiances are chosen as the reference. The differences between the UARS SUSIM (version 19) and SOLSTICE Lyman α irradiances are now only a few percent as shown in Figure 1. Prior to 1993 the SOLSTICE values are, on average, 2% lower than the

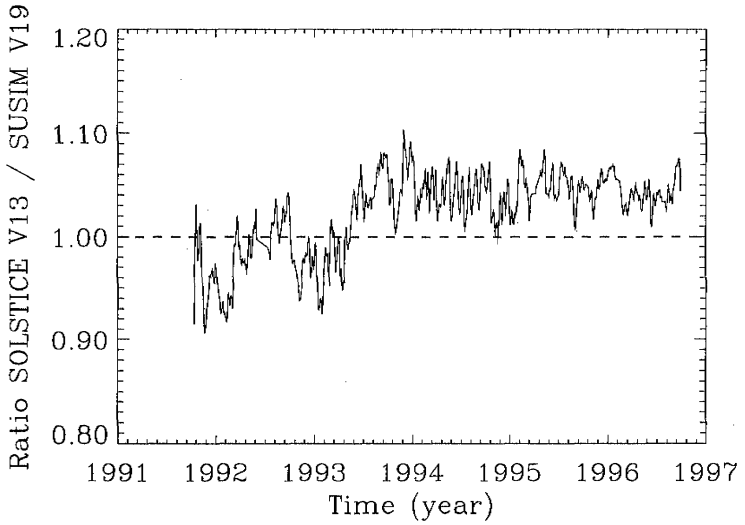

Figure 1. Solar Ultraviolet Spectral Irradiance Monitor (SUSIM) – SOLar STellar Irradiance Comparison Experiment (SOLSTICE) Lyman α comparison. The average ratio changes from 0.98 to 1.04 during 1993.

SUSIM values. After 1993 the SOLSTICE values are, on average, 4% higher than the SUSIM values. These differences are instrument and calibration artifacts. We considered using the average of SUSIM and SOLSTICE data as the reference but decided that the reference time series would be more consistent using data from a single instrument. As compared to a factor of 2 for solar cycle variability, the differences of a few percent between SOLSTICE and SUSIM would not significantly alter the results presented here.

An important difference between this new composite Lyman α time series and *Woods and Rottman*'s [1997] and *Tobiska et al.'s* [1997] time series is that the SOLSTICE version 13 data products are now used. The two previous results used the SOLSTICE version 9 data products. The SOLSTICE version 13 data processing software has several algorithm enhancements. The four algorithm changes that affect the Lyman α irradiance the most are (1) a new, time-dependent, wavelength-scale correction, (2) a new, time-dependent, field of view (FOV) correction, (3) an improved, overflow counter correction, and (4) an improved algorithm to calculate the line integral. The ratio of the SOLSTICE Lyman α version 9 to version 13 is shown in Figure 2. The primary difference is from the new wavelength-scale correction. The second most important improvement is from the new FOV correction. The improved overflow counter correction reduces day-to-day noise but does not contribute to the long-term

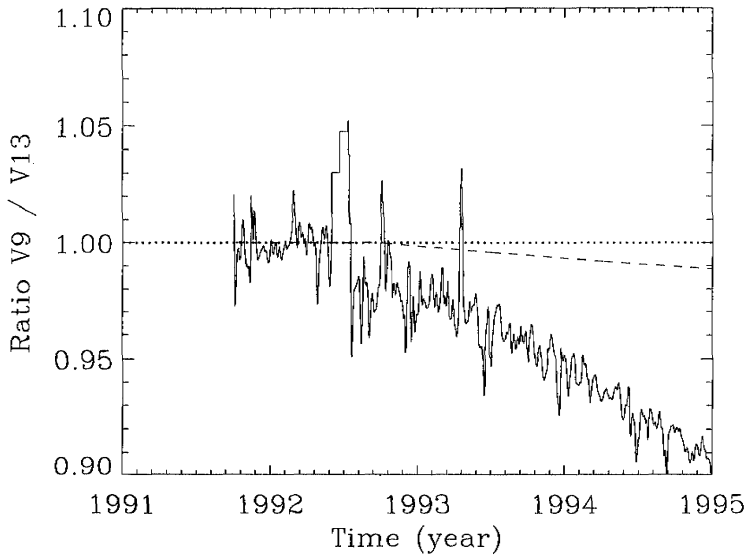

Figure 2. Comparison of SOLSTICE Lyman α version 9 to version 13. The dashed line is the new field of view correction. The remaining difference is primary from the new wavelength-scale correction.

trend. The new line integral algorithm improves the accuracy of deriving the irradiance into 1-nm intervals, but it does not contribute to the long-term trend.

The new wavelength-scale correction is needed to account for a slow drift of the SOLSTICE grating drive encoder electronics. This encoder degradation was first discovered from examination of changes in solar line widths; some were slowly growing wider, and some were slowly growing narrower. Through the comparisons of daily spectra to a reference solar spectrum early in the UARS mission, the grating drive encoder signal was found to be slowly drifting, and a simple correction for the encoder degradation is now applied. The new wavelength-scale correction algorithm has yielded line widths that remain constant over the mission. This wavelength-scale correction is the most significant improvement over the previous work as it affected the long-term trend by several percent.

The FOV correction is a new calibration for the "hole" seen in the SOLSTICE G channel (119-180 nm) FOV maps [*Woods et al.*, 1999]. This FOV correction is largest for the longer wavelengths of the G channel; nevertheless, this correction is also important for the SOLSTICE Lyman α time series. The FOV correction for Lyman α is about a 1-2% correction and is shown in Figure 2 as the dashed line.

The improvements in the overflow counter correction algorithm, which is used when detector counts exceed the 16-bit hardware counter, has yielded lower day-to-day noise in the SOLSTICE Lyman α time series.

The fourth algorithm improvement is the change from a numerical integration to an analytical integration using basis spline functions fitted to the data [*Lawson and Hanson*, 1974; *de Boor*, 1978]. The basis spline integrations are done for both the line integrations, such as for the Lyman α emission, and the 1-nm intervals used in the UARS Level 3BS data products. The use of analytical integrations has improved the accuracy of creating 1-nm intervals for the SOLSTICE Level 3BS data product. With the old numerical integration algorithm, there were differences of a few percent between the Lyman α irradiance represented by the 121-122 nm interval irradiance and the irradiance from a Gaussian fit to the Lyman α line. Now the Lyman α irradiances extracted the two different ways are in agreement using the new analytical integration algorithm.

3. Lyman α Proxy Models

Models of solar irradiance are used primarily for atmospheric studies for time periods when measurements are not available. A commonly used solar irradiance model for upper atmospheric studies is *Hinteregger et al.*'s [1981] proxy model. This model and other proxy models employ empirically derived relationships of solar irradiance at one wavelength relative to an index of solar variability that is available on an almost daily basis over many years. Improvements in modeling the solar Lyman α irradiance variability can be obtained by specifying the irradiance as a function of the distribution of quiet and magnetic solar surface features, such as was done by *Lean and Skumanich* [1983] and *Worden* [1996]. Both of their models parameterize the solar irradiance as three components: quiet Sun, active network, and plage areas whereby the areas of each component are derived from Ca II K solar images. A more detailed description of these three components and the relationship of these components to the empirical proxy models is given in section 6. A more physical model of the Lyman α irradiance is the radiative transfer calculations using semiempirical models of the solar atmospheric structure (density and temperature), such as those by *Vernazza et al.* [1981] and *Fontenla et al.* [1999]. In *Fontenla et al.'s* [1999] model, solar images are used to identify seven components of the solar atmosphere (e.g., cell interior, network, and plage), and then an emission's source function is calculated using seven static models of the solar atmosphere. However, the image analyses have only been done over a limited time period and thus are difficult to extend back to the time of the AE-E mission and before. Therefore the simpler proxy model approach is applied here but with some improvements over previous proxy models.

The validity of a proxy model is strongly dependent on the validity of the proxy over its entire time range and on the physical processes connecting the proxy emission and the Lyman α emission within the solar atmosphere. The Lyman α radiation is formed in the chromosphere and transition region of the solar atmosphere, so the most appropriate solar proxies should likewise have a dominant contribution from these regions. In addition, the time series of the proxies need to be long enough to overlap AE-E, SME, and UARS. The three indices used here for Lyman α proxy modeling are the $F10.7$, Mg C/W, and He EW. The solar $F10.7$ measurement has the longest duration dating back to 1947. The two primary sources in the solar atmosphere for the 10.7-cm radio flux are the free-free electron emission (bremsstrahlung) throughout the chromosphere, transition region, and lower corona and gyroresonant absorption in strong magnetic fields in the transition region and corona [*Tapping*, 1987]. While the daily $F10.7$ is better correlated with coronal emissions than with the Lyman α emission, both the 81-day average $F10.7$ and the square root of $F10.7$ have a good correlation with the Lyman α emission, better than 0.95. Because the correlation with the square root of $F10.7$ is better than the correlation with $F10.7$, the square root of $F10.7$ is used here solely as an empirical improvement. The He EW measurement is representative of the chromosphere and transition region but is also sensitive to coronal holes. The Mg C/W is representative of the chromosphere.

The empirical fits of the UARS Lyman α irradiance measurements to the three solar indices yield the following models for the solar Lyman α irradiance:

$$E = A + C_L P_{81} + C_S \left(P - P_{81}\right), \quad \text{(1a)}$$

$$E_{He} = 1.1764 + 0.05668\, He_{81} + 0.04032 \left(He - He_{81}\right), \quad \text{(1b)}$$

$$E_{Mg} = -31.68 + 133.7\, Mg_{81} + 79.52 \left(Mg - Mg_{81}\right), \quad \text{(1c)}$$

$$E_{F10} = 0.5839 + 0.3554 \sqrt{F10_{81}} + 0.1730 \left(\sqrt{F10} - \sqrt{F10_{81}}\right). \quad \text{(1d)}$$

The proxy variables P are labeled He for the NSO He-1083 nm EW, Mg for the NOAA Mg II core-to-wing ratio, and $\sqrt{F10}$ for the square root of $F10.7$. The irradiance E is given in units of 10^{11} photons s^{-1} cm^{-2}. The variables, or indices, with the "81" subscript are the daily proxy values smoothed over a period of 81 days. Data gaps in the proxies, which pose a problem for the 81-day smoothing function, are filled by interpolation if the gap is smaller than 6 days or by fast Fourier transform analysis if the gap is larger [*Worden*, 1996]. These proxy models are derived empirically using the common method of multiple linear regression. The SOLSTICE Mg II core-to-wing ratio is also used for analysis later, and the SOLSTICE Mg

proxy is related to the NOAA Mg proxy as $Mg_{NOAA} = 0.1914 + 0.3787\ Mg_{SOLSTICE}$. The three terms in (1) represent a constant term (conceptually, the quiet Sun), long-term variation, and short-term variation. The third coefficient, C_S, is the sensitivity to the short-term variation, predominantly from 27-day solar rotation. Likewise, the second coefficient, C_L, is the sensitivity to the long-term variation. *Lean and Skumanich* [1983] and *Worden* [1996] have shown for chromospheric emissions that the short-term variation is due mostly to plage modulated by solar rotation and that the long-term variation is due mostly to variations in both plages and active network. These simple three-component proxy models were motivated by the more physical three-component models of irradiance variability by *Lean and Skumanich* [1983] and *Worden* [1996] in which they used Ca II K images to derive plage and active network areas as the main variables in their models. The quiet Sun (solar minimum) irradiance from (1) is 3.55 x 10^{11} photons s^{-1} cm^{-2} using the 81-day-smoothed solar minimum values for the proxies: He=He_{81}=42, Mg=Mg_{81}=0.26, and $F10$=$F10_{81}$=70.

These proxy model coefficients are similar to, but consistently different from, the equivalent model coefficients given by *Woods and Rottman* [1997]. Because the new SOLSTICE version 13 Lyman α irradiance has a higher solar minimum value than that extrapolated using SOLSTICE version 9 data, the constant coefficients are higher than those given by *Woods and Rottman* [1997], and the long-term variation coefficients are lower than *Woods and Rottman's* [1997] results. As expected, the 27-day variation coefficients are more consistent with previous results as they are not sensitive to the long-term trend.

As a validation check for these models, we also derive the model parameters for the SOLSTICE Lyman α irradiance over shorter time periods. If the model parameters are consistent by using different SOLSTICE data periods, then one could conclude that the SOLSTICE data set is consistent throughout its mission and that the proxy model is a reasonable representation at different stages of solar variability. The lifetime of a plage decaying into active network is one to three solar rotations [*Foukal*, 1998], and the lifetime of active network diffusing into the quiet network is possibly several solar rotations. So a period of nine solar rotations, 243 days, is chosen for this validation analysis. The three parameters, A, C_L, and C_S, are shown in Figure 3, using the Mg proxy model over a 243-day period every 27 days. These 243-day fitting results indicate that the short-term parameter, C_S, varies 17% over the SOLSTICE mission; however, the constant coefficient, A, and the long-term parameter, C_L, vary 75 and 50%, respectively. *Barth et al.* [1990] found similar variation of the coefficients for a two-component Lyman α model in that the coefficients changed by a factor of 1.6 during different phases of the solar cycle. These 243-day A and C_L

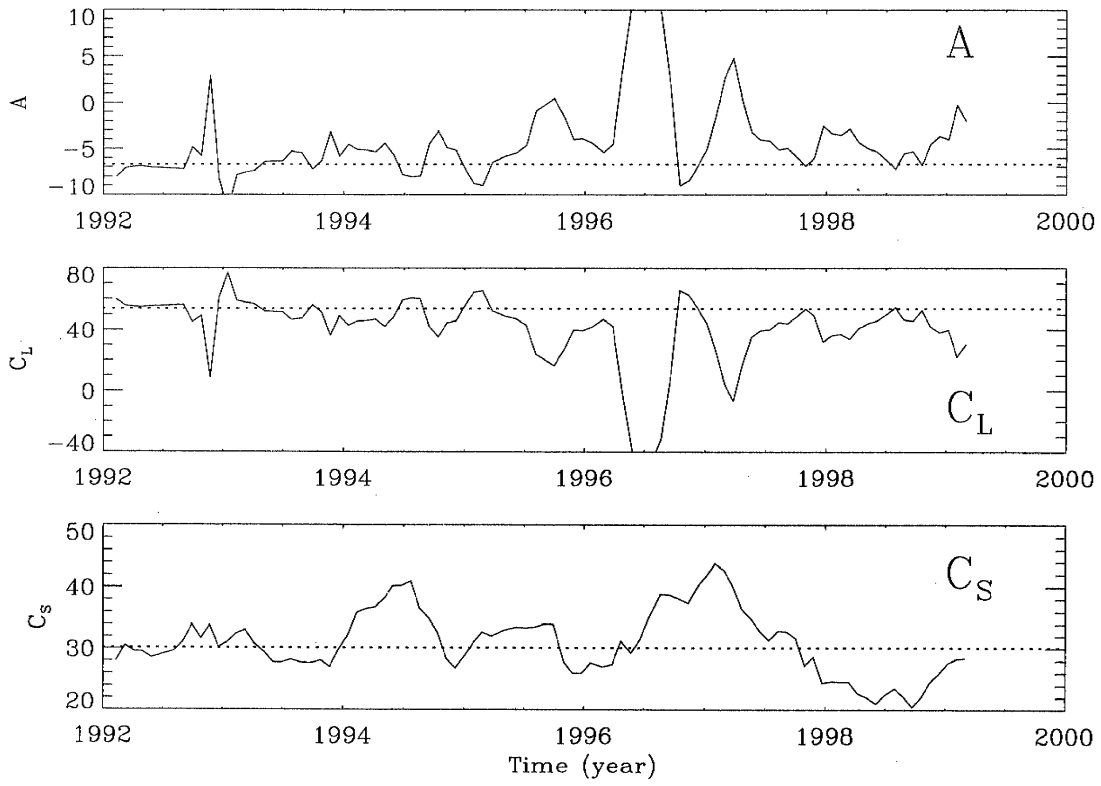

Figure 3. Proxy model parameters for 243-day periods. The parameters for the Mg proxy model are fitted for a 243-day period every 27 days. The times when A and C_L change the most are the times when there is little solar activity or when the solar activity level changed rapidly. The dotted lines are the values for the model parameters using the entire SOLSTICE mission. These values are not the same as equation (1) values because the SOLSTICE Mg core-to-wing ratio (Mg C/W index) is used here instead of the NOAA Mg C/W index.

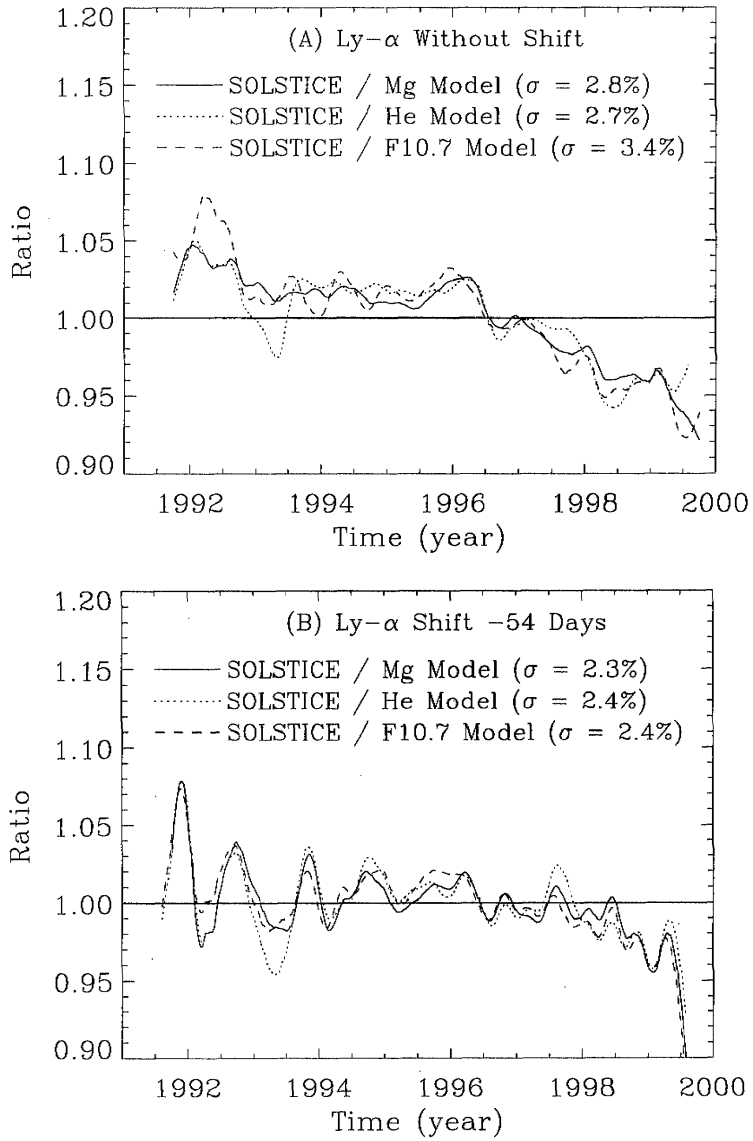

Figure 4. Proxy model comparison for UARS SOLSTICE Lyman α. (a) Model comparisons with no shifts between the proxies and Lyman α. There is a downward trend after solar minimum (1996) for this comparison. (b) Model shows model comparisons with SOLSTICE Lyman α shifted backward (earlier) by 54 days (two solar rotations). The downward trend is reduced with this 54 day shift, and this change is discussed in section 6.5. The standard deviation (σ) of the fit is shown in parentheses.

parameters are consistent with the values derived using the entire SOLSTICE data set (dotted lines in Figure 3). Note that these values are not the same as equation (1) values, because the SOLSTICE Mg C/W index is used here instead of the NOAA Mg C/W index. The times of little solar variability as in 1996 and the times of rapid changes as in 1993 are when the 243-day A and C_L parameters deviate the most from the mean value. The He proxy model shows very similar results when it is analyzed in the same way, but the $F10.7$ proxy model shows a factor of 2 larger spread of the parameters in doing the 243-day fitting. Because the 243-day parameters do not show any long-term trend, there does not appear to be any significant instrument artifacts remaining in the SOLSTICE data set. We also conclude that the Mg and He proxies seem the more appropriate proxies to represent the solar Lyman α variability.

The major limitations for the proxy models are the uncertainties in the proxies themselves, the uncertainties in the solar irradiance data used to derive empirically the model coefficients, and intrinsic differences between the physical regions and mechanisms that emit the radiation for the proxy and at Lyman α. The uncertainties in the proxies are estimated from the day-to-day noise in the proxy and the difference in solar minimum values, assuming that all solar minimum

values should be the same. The day-to-day noise is calculated as the standard deviation of the difference between the proxy and a 3-day-smoothed proxy. This calculation may also include true solar variability, but the value is small anyway. The day-to-day noise is 1.3, 0.3, and 0.9% for He, Mg, and $\sqrt{F10}$, respectively. The difference between the solar minimum values averaged over a year is 6.3, 0.1, and 2.9% for He, Mg, and $\sqrt{F10}$, respectively. The larger difference for the He proxy may be related to the change of the He EW instrument in 1993. Therefore we estimate the proxy uncertainties to be 6, 0.3, and 3% for He, Mg, and $\sqrt{F10}$, respectively. From validation with UARS SUSIM and analysis of the SOLSTICE irradiance algorithms, the uncertainty for the UARS Lyman α irradiance is 5% [*Woods et al.*, 1996]. An estimate for the intrinsic difference between the source region of the index and the source region of Lyman α is the standard deviation (1-σ) of the difference between the model prediction and the UARS measurements, being 2.7, 2.3, and 3.0% for the He, Mg, and $F10$ models, respectively (see Figure 4a). This uncertainty should be considered a lower limit rather than the best approximation for the intrinsic difference between the index and Lyman α source regions. Combining these uncertainties, the expected uncertainty for the proxy model predictions is 8, 6, and 7% for the He, Mg, and $F10$ models, respectively. A validation check on the total uncertainty of the proxy model predictions is the temporal difference, not including the systematic offset, of the model predictions to the SME measurements, being 2.8, 3.2, and 4.0% for the He, Mg, and $F10$ models, respectively (see Figure 5a). Hence an uncertainty of 10% appears reasonable to adopt for the proxy model predictions. While additional analysis or different algorithms might provide a proxy model with an uncertainty better than 10%, the uncertainty of the UARS irradiances will remain the limiting factor for the proxy model uncertainty.

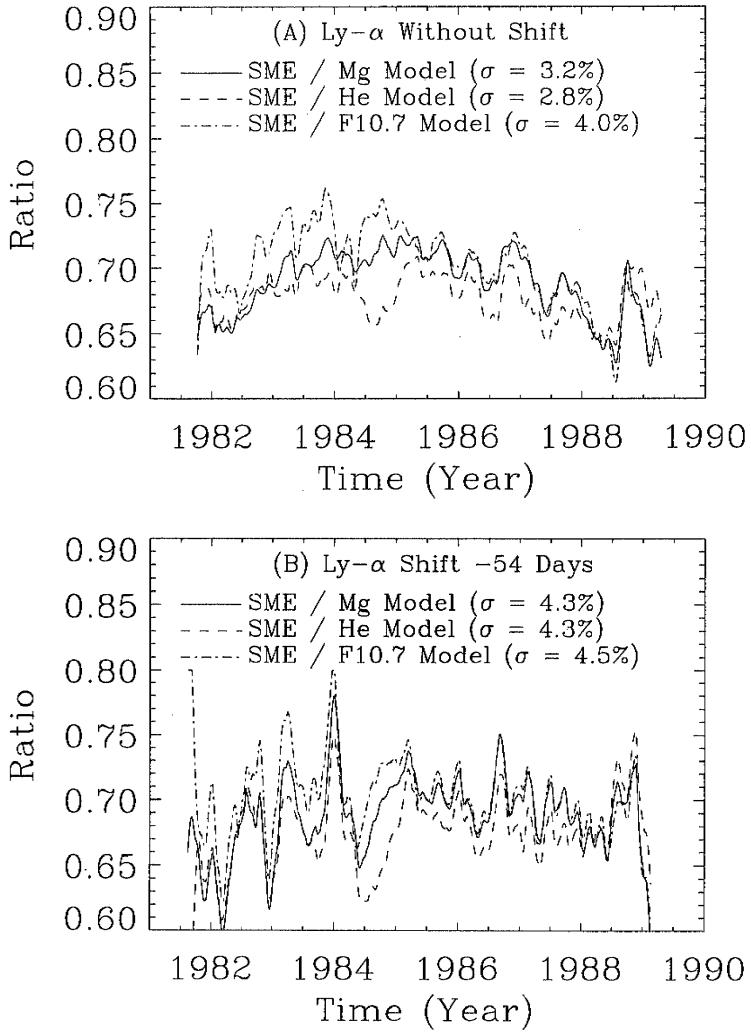

Figure 5. Proxy model comparison for Solar Mesospheric Explorer (SME) Lyman α. (a) Model shows model comparisons with no shifts between the proxies and Lyman α. There is a downward trend after solar minimum (1986) for this comparison. (b) Model shows model comparison with the SME data shifted backward (earlier) by 54 days (two solar rotations). The downward trend is reduced with this 54-day shift, and this change is discussed in section 6.5. The standard deviation (σ) of the fit is shown in parentheses.

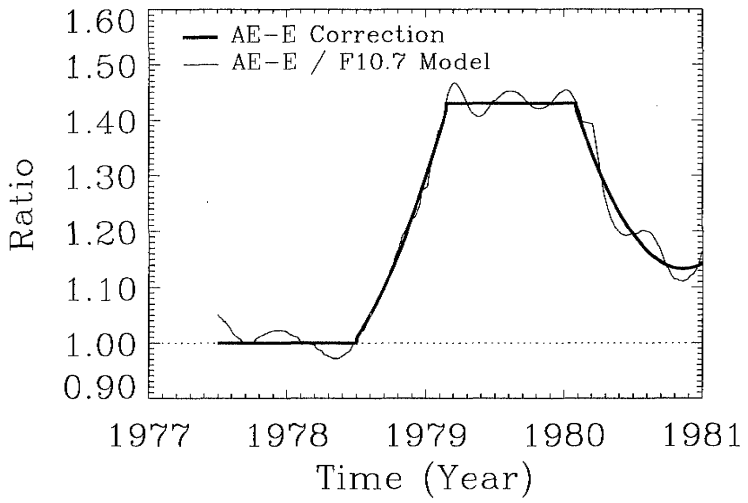

Figure 6. Proxy model comparison for AE-E Lyman α. The correction for the AE-E Lyman α is a time-dependent function shown as the thick line.

Considering that the solar cycle Lyman α variability is about a factor of 2, the proxy model uncertainty of 10% is quite adequate for modeling the long-term solar variability.

4. Composite Lyman α Time Series

A composite Lyman α time series is formed using the UARS SOLSTICE Lyman α measurements, adjusted measurements from AE-E and SME, and proxy model predictions to fill the data gaps and to extend the time series back to 1947. We use the UARS Lyman α data as our fundamental reference both for the absolute registration of this time series in order to establish adjustments for the AE-E and SME data and for the development of the proxy models of the solar Lyman α irradiance.

The scaling factors for the SME and AE-E Lyman α irradiance are derived assuming that the UARS SOLSTICE proxy models are valid and can be extrapolated to times prior to the UARS mission. The average ratios of the SME data to the proxy models shown in Figure 5a are 0.69, 0.68, and 0.70 for the Mg, He, and *F*10.7 models, respectively. The standard deviation for these ratios is only 3%, mainly because the ratios do not have a strong variation with time. Because the degradation of the SME solar instrument is a small correction at Lyman α, this result implies that the SME solar instrument was relatively stable during its mission. A scaling factor of 0.69 that is independent of time is adopted for scaling the SME Lyman α irradiances. This value is the average of the proxy model ratios presented in Figure 5a. The SME Lyman α irradiances, divided by this scaling factor, are increased and become consistent with the SOLSTICE Lyman α irradiance values.

On the other hand, the comparison of the AE-E Lyman α irradiances to the proxy models shows significant variations from the mean difference. *Fukui* [1990] argues that the 1979 anomaly in the AE-E Lyman α irradiances is a real solar effect because two AE-E channels recorded the same variation in the Lyman α irradiances and a similar, but smaller, variation was observed in the AE-E Lyman β emission. While their study and conclusions should not lightly be dismissed, ground-based solar measurements do not suggest an obvious solar mechanism that could explain the 45% anomaly of the AE-E irradiances. From our experience with photomultiplier tube (PMT) detectors, we have seen changes in PMT gain that can both go up or go down as the high-voltage power supply (HVPS) degrades, as the temperature of the HVPS changes, or as the 28-V input supply (battery-solar cells) changes levels. *Fukui* [1990] does not consider these possible effects; nonetheless, these effects would probably have affected other AE-E channels in a similar manner. Another possibility is that the contamination levels changed. *Fukui* [1990] indicates that the AE-E detectors are most sensitive to contamination at Lyman α and longer wavelengths, because the response at Lyman α dropped by a factor of 5 during the first several months of the AE-E mission while the response at shorter wavelengths changed by less than 30%. *Fukui* [1990] speculates that this decrease in Lyman α responsivity is due to outgassing of the photocathode impurities from the detector. Impurities tend to migrate to the colder components, so it is conceivable that some of the impurities could return to the detectors if the detectors were colder during the anomaly period. These ideas are only speculations on how the AE-E instrument might have degraded during the anomaly period. In order for the AE-E Lyman α measurements to be consistent with the proxy models, the AE-E instrument responsivity is assumed, without proof, to change during the anomaly period. Consequently, a time-dependent scaling factor for the AE-E Lyman α irradiances is adopted as shown in Figure 6. These scaling factors, *f*, for the AE-E Lyman α irradiances include constant offsets plus quadratic fits with time, *t*, in fractional years, as listed in (2).

$$1977.5\text{-}1978.5 \qquad f = 1.0 \tag{2a}$$

$$1978.5\text{-}1979.145 \qquad f = 2365.15 - 60.615\,t + 0.38852\,t^2 \tag{2b}$$

$$1979.145\text{-}1980.085 \qquad f = 1.43 \tag{2c}$$

$$1980.085\text{-}1981 \qquad f = 3153.56 - 77.978\,t + 0.48222\,t^2 \tag{2d}$$

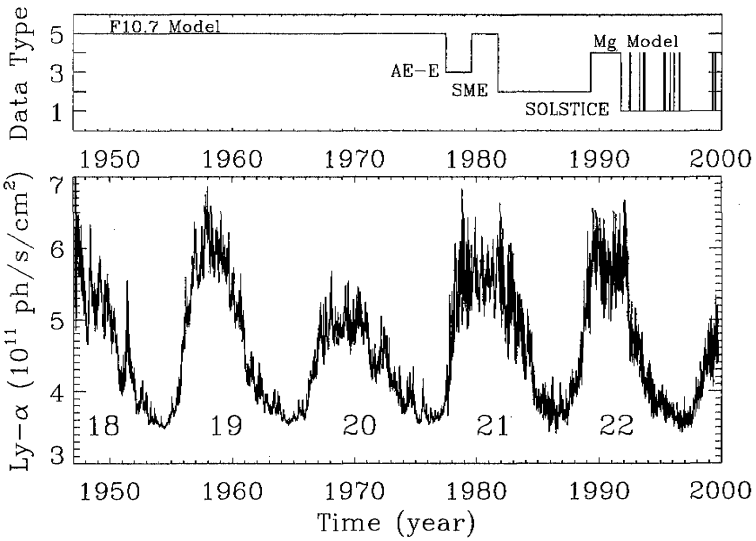

Figure 7. Composite solar Lyman α time series. The top panel shows the source for the Lyman α irradiance shown in the bottom panel. The sources are (1) UARS SOLSTICE, (2) SME, (3) AE-E, (4) Mg proxy model, and (5) *F*10.7 proxy model.

These scaling factors for SME and AE-E are higher than the scaling factors given by *Woods and Rottman* [1997] and *Tobiska et al.* [1997], because the UARS SOLSTICE version 13 Lyman α irradiances have a higher solar minimum value than the extrapolated value from the SOLSTICE version 9 data. Because the UARS mission has now observed both solar maximum and minimum conditions, these scaling factors are not expected to change significantly as the UARS mission extends its solar observations into the next solar cycle.

The composite Lyman α time series is shown in Figure 7 along with an indicator of the source of the values in the time series: (1) UARS SOLSTICE Lyman α measurements, (2) scaled SME Lyman α measurements, (3) scaled AE-E Lyman α measurements, (4) Mg II C/W model predictions used between SME and UARS observations and for filling SOLSTICE data gaps, and (5) *F*10.7 model predictions used prior to SME observations. The Mg II C/W proxy is considered the more appropriate proxy for chromospheric emissions, but the *F*10.7 proxy is utilized in order to extend the composite time series back to 1947. For data gaps of less than 5 days the measurements are linearly interpolated to fill the data gaps. For longer data gaps the proxy models are used to fill the data gaps. The composite time series is then smoothed by 3 days to help reduce day-to-day noise and to make transitions smooth from one data source to another.

The many rocket measurements of the solar Lyman α irradiance from 1949 to 1998 serve as a validation for the composite Lyman α time series. The comparison of 59 rocket measurements [*Vidal-Madjar*, 1977; *Mount and Rottman*, 1983, 1985; *Rottman*, 1981; *Van Hoosier et al.*, 1988; *Woods and Rottman*, 1990] to the composite time series is shown in Figure 8. The 42 Lyman α measurements from *Vidal-Madjar*'s [1977] review of the solar Lyman α irradiance are indicated by the asterisks. *Vidal-Madjar* [1977] had concluded that the Lyman α irradiance ranged from 2 to 4 x 10^{11} photons s^{-1} cm^{-2} with an uncertainty of 30%. These earlier rocket measurements, except for one measurement in 1955, do not confirm our composite Lyman α time series. These values are a factor of ~1.7 smaller than our composite Lyman α time series. *Vidal-Madjar* [1977] noted that some atmospheric and cometary studies suggest an increase of the solar extreme ultraviolet (EUV) and Lyman α irradiances by a factor of 2. While our composite Lyman α time series support this factor of 2 increase of *Vidal-Madjar*'s [1977] values, it is difficult to resolve this factor of 2 when both the uncertainty of these solar Lyman α irradiance measurements and the uncertainty of the atmospheric model predictions were estimated at 30% or larger [*Vidal-Madjar*, 1977]. However, there are some concerns about the use of tungsten photodiodes for the calibration of the earlier solar instruments (W. Neupert, private communication, 1993) because *Canfield et al.* [1973] found that the photoelectric yield of tungsten could change by as much as a factor of 2 above 100 nm based on its surface cleanliness and that these older photodiodes could have a variation in sensitivity across the photodiode by as much as 50%. It seems possible that these original calibration tungsten photodiodes were easily contaminated because only oil-based pumps were used in those times. If so, then these earlier solar measurements are expected to have low values. For these older measurements we assume an uncertainty of 80%, being the combination of the typical 30% measurement uncertainty [*Vidal-Madjar*, 1977] and a 50% uncertainty for the possible systematic error of the tungsten photodiode calibrations.

The more recent rocket measurements from 1976 to 1998 provide a better confirmation of our composite Lyman α irradiances. There are eight measurements that agree with our composite Lyman α irradiances, and the other six measurements are more consistent with the lower values reported by *Vidal-Madjar* [1977]. The SME Lyman α irradiance was calibrated to the 1982 rocket measurement, shown as the large diamond in Figure 8; therefore the SME Lyman α values are expected to be lower than the composite time series. The uncertainties of the rocket Lyman α irradiance measurements are estimated to be ~30-40% [*Rottman*, 1981; *Woods and Rottman*, 1990]. There are several